Optical properties of light absorbing carbon aggregates mixed with sulfate: assessment of different model geometries for climate forcing calculations

Michael Kahnert,[1,2,*] **Timo Nousiainen,**[3] **Hannakaisa Lindqvist,**[3] **and Martin Ebert**[4]

[1] *Swedish Meteorological and Hydrological Institute (SMHI), Research Department, Folkborgsvägen 1, SE-601 76 Norrköping, Sweden*

[2] *Chalmers University of Technology, Department of Earth and Space Science, SE-412 96 Gothenburg, Sweden*

[3] *Department of Physics, P. O. Box 48, FI-00014 University of Helsinki, Finland*

[4] *Technical University of Darmstadt, Institute for Applied Geosciences, Schnittspahnstraße 9, DE-64287 Darmstadt, Germany*

[*] *michael.kahnert@smhi.se*

Abstract: Light scattering by light absorbing carbon (LAC) aggregates encapsulated into sulfate shells is computed by use of the discrete dipole method. Computations are performed for a UV, visible, and IR wavelength, different particle sizes, and volume fractions. Reference computations are compared to three classes of simplified model particles that have been proposed for climate modeling purposes. Neither model matches the reference results sufficiently well. Remarkably, more realistic core-shell geometries fall behind homogeneous mixture models. An extended model based on a core-shell-shell geometry is proposed and tested. Good agreement is found for total optical cross sections and the asymmetry parameter.

OCIS codes: (290.5850) Scattering, particles; (010.1110) Aerosols; (010.1310) Atmospheric scattering; (290.5825) Scattering theory; (290.1350) Backscattering; (010.1290) Atmospheric optics.

References and links

1. M. Z. Jacobson, "Strong radiative heating due to the mixing state of black carbon in atmospheric aerosols," Nature **409**, 695–697 (2001).
2. P. Forster, V. Ramaswamy, P. Artaxo, T. Berntsen, R. Betts, D. W. Fahey, J. Haywood, J. Lean, D. C. Lowe, G. Myhre, J. Nganga, R. Prinn, G. Raga, M. Schulz, and R. Van Dorland, "Changes in atmospheric constituents and in radiative forcing." in *Climate Change 2007: The Physical Science Basis*, S. Solomon, D. Qin, M. Manning, Z. Chen, M. Marquis, K. B. Averyt, M. Tignor, and H. L. Miller, eds. (Cambridge University Press, 2007), Contribution of Working Group I to the Fourth Assessment Report of the Intergovernmental Panel on Climate Change.
3. V. Ramanathan and G. Carmichael, "Global and regional climate changes due to black carbon," Nat. Geosci. **1**, 221–227 (2008).
4. K. Adachi, S. H. Chung, H. Friedrich, and P. R. Buseck, "Fractal parameters of individual soot particles determined using electron tomography: Implications for optical properties," J. Geophys. Res. **112**, D14202 (2007).
5. A. R. Jones, "Light scattering in combustion," in *Light Scattering Reviews*, A. Kokhanovsky, ed., (Springer, 2006).
6. M. Kahnert, "Modelling the optical and radiative properties of freshly emitted light absorbing carbon within an atmospheric chemical transport model," Atmos. Chem. Phys. **10**, 1403–1416 (2010).

#163542 - $15.00 USD Received 22 Feb 2012; revised 12 Apr 2012; accepted 12 Apr 2012; published 18 Apr 2012

7. T. C. Bond and R. W. Bergstrom, "Light absorption by carbonaceous particles: an investigative review," Aerosol Sci. Technol. **40**, 27–67 (2006).
8. M. Kahnert, "On the discrepancy between modelled and measured mass absorption cross sections of light absorbing carbon aerosols," Aerosol Sci. Technol. **44**, 453–460 (2010).
9. D. W. Mackowski and M. I. Mishchenko, "Calculation of the T matrix and the scattering matrix for ensembles of spheres," J. Opt. Soc. Am. A **13**, 2266–2278 (1996).
10. M. Kahnert, "Numerically exact computation of the optical properties of light absorbing carbon aggregates for wavelength of 200 nm V 12.2 μm," Atmos. Chem. Phys. **10**, 8319–8329 (2010).
11. N. Riemer, H. Vogel, and B. Vogel, "Soot aging time scales in polluted regions during day and night," Atmos. Chem. Phys. **4**, 1885–1893 (2004).
12. S. Tsyro, D. Simpson, L. Tarrasón, Z. K. K. Kupiainen, C. Pio, and K. E. Yttri, "Modelling of elemental carbon over Europe," J. Geophys. Res. **112**, D23S19 (2007).
13. B. Croft, U. Lohmann, and K. von Salzen, "Black carbon aging in the Canadian Centre for climate modelling and analysis atmospheric general circulation model," Atmos. Chem. Phys. **5**, 1383–1419 (2005).
14. R. J. Park, D. J. Jacob, P. I. Palmer, A. D. Clarke, R. J. Weber, M. A. Zondlo, F. L. Eisele, A. R. Bandy, D. C. Thornton, G. W. Sachse, and T. C. Bond, "Export efficiency of black carbon aerosol in continental outflow: global implications," J. Geophys. Res. **110**, D11205 (2005).
15. J. Wilson, C. Cuvelier, and F. Raes, "A modeling study of global mixed aerosol fields," J. Geophys. Res. **106**, 34081–34108 (2001).
16. K. Adachi and P. R. Buseck, "Internally mixed soot, sulfates, and organic matter in aerosol particles from Mexico City," Atmos. Chem. Phys. **8**, 6469–6481 (2008).
17. M. Schnaiter, H. Horvath, O. Möhler, K.-H. Naumann, H. Saathoff, and O. W. Schöck, "UV-VIS-NIR spectral optical properties of soot and soot-containing aerosols," J. Aerosol Sci. **34**, 1421–1444 (2003).
18. J. Hallett, J. G. Hudson, and C. F. Rogers, "Characterization of combustion aerosols for haze and cloud formation," Aerosol Sci. Technol. **10**, 70–83 (1989).
19. I. Colbeck, L. Appleby, E. J. Hardman, and R. M. Harrison, "The optical properties and morphology of cloud-processed carbonaceous smoke," J. Aerosol Sci. **21**, 527–538 (1990).
20. G. Ramachandran and P. C. Reist, "Characterization of morphological changes in agglomerates subject to condensation and evaporation using multiple fractal dimensions," Aerosol Sci. Technol. **23**, 431–442 (1995).
21. S. Nyeki and I. Colbeck, "Fractal dimension analysis of single, in-situ, restructured carbonaceous aggregates," Aerosol Sci. Technol. **23**, 109–120 (1995).
22. C. M. Sorensen and G. M. Roberts, "The prefactor of fractal aggregates," J. Colloid. Interface Sci. **186**, 447–452 (1997).
23. L. H. van Poppel, H. Friedrich, J. Spinsby, S. H. Chung, J. H. Seinfeld, and P. R. Buseck, "Electron tomography of nanoparticle clusters: Implications for atmospheric lifetimes and radiative forcing of soot," Geophys. Res. Lett. **32**, L24811 (2005).
24. P. Chýlek, G. Videen, D. J. W. Geldart, J. S. Dobbie, and H. C. W. Tso, "Effective medium approximations for heterogeneous particles," in *Light Scattering by Nonspherical Particles*, M. I. Mishchenko, J. W. Hovenier, and L. D. Travis, eds. (Academic Press, 2000), pp. 274–308.
25. G. Videen and P. Chýlek, "Scattering by a composite sphere with an absorbing inclusion and effective medium approximations," Opt. Commun. **158**, 1–6 (1998).
26. M. Z. Jacobson, "A physically-based treatment of elemental carbon optics: Implications for global direct forcing of aerosols," Geophys. Res. Lett **27**, 217–220 (2000).
27. T. C. Bond, G. Habib, and R. W. Bergstrom, "Limitations in the enhancement of visible light absorption due to mixing state," J. Geophys. Res. **111**, D20211 (2006).
28. M. Kocifaj and G. Videen, "Optical behavior of composite carbonaceous aerosols: DDA and EMT approaches," J. Quant. Spectrosc. Radiat. Transfer **109**, 1404–1416 (2008).
29. K. A. Fuller, "Scattering and absorption cross sections of compounded spheres III. spheres containing arbitrarily located spherical inhomogeneities," J. Opt. Soc. Am. A **12**, 893–904 (1995).
30. K. A. Fuller, W. C. Malm, and S. M. Kreidenweis, "Effects of mixing on extinction by carbonaceous particles," J. Geophys. Res. **104**, 15941–15954 (1999).
31. K. Adachi, S. Chung, and P. R. Buseck, "Shapes of soot aerosol particles and implications for their effects on climate," J. Geophys. Res. **115**, D15206 (2010).
32. A. Worringen, M. Ebert, T. Trautmann, S. Weinbruch, and G. Helas, "Optical properties of internally mixed ammonium sulfate and soot particles—a study of individual aerosol particles and ambient aerosol populations," Appl. Opt. **47**, 3835–3845 (2008).
33. E. M. Purcell and C. R. Pennypacker, "Scattering and absorption of light by nonspherical dielectric grains," Astrophys. J. **186**, 705–714 (1973).
34. L. Liu and M. I. Mishchenko, "Scattering and radiative properties of complex soot and soot-containing aggregate particles," J. Quant. Spectrosc. Radiat. Transfer **106**, 262–273 (2007).
35. H. Chang and T. T. Charalampopoulos, "Determination of the wavelength dependence of refractive indices of flame soot," Proc. R. Soc. Lond. Ser. A **430**, 577–591 (1990).

#163542 - $15.00 USD Received 22 Feb 2012; revised 12 Apr 2012; accepted 12 Apr 2012; published 18 Apr 2012

36. M. Hess, P. Koepke, and I. Schult, "Optical properties of aerosols and clouds: the software package OPAC," Bull. Am. Met. Soc. **79**, 831–844 (1998).
37. B. T. Draine and P. J. Flatau, "Discrete-dipole approximation for scattering calculations," J. Opt. Soc. Am. A **11**, 1491–1499 (1994).
38. T. Rother, *Electromagnetic Wave Scattering on Nonspherical Particles* (Springer, 2009).
39. M. Kahnert and T. Rother, "Modeling optical properties of particles with small-scale surface roughness: combination of group theory with a perturbation approach," Opt. Express **19**, 11138–11151 (2011).
40. D. Gutkowicz-Krusin and B. T. Draine, *Propagation of electromagnetic waves on a rectangular lattice of polarizable points*, Tech. rep., http://arxiv.org/abs/astro-ph/0403082 (2004).
41. E. Zubko, K. Muinonen, Y. Shkuratov, G. Videen, and T. Nousiainen, "Scattering of light by roughened Gaussian random particles," J. Quant. Spectrosc. Radiat. Transfer **106**, 604–615 (2007).
42. M. I. Mishchenko, , L. D. Travis, and A. A. Lacis, *Scattering, Absorption, and Emission of Light by Small Particles* (Cambridge University Press, 2002).
43. O. B. Toon and T. P. Ackermann, "Algorithms for the calculation of scattering by stratified spheres," Appl. Opt. **20**, 3657–3660 (1981).
44. Z. S. Wu and Y. P. Wang, "Electromagnetic scattering for multilayered sphere: recursive algorithms," Radio Sci. **26**, 1393–1401 (1991).
45. J. C. Maxwell-Garnett, "Colours in metal glasses and in metallic films," Philos. Trans. R. Soc. Ser. A **203**, 385–420 (1904).
46. D. A. G. Bruggemann, "Berechnung verschiedener physikalischer Konstanten von heterogenen Substanzen. 1. Dielektrizitätskonstanten und Leitfähigkeiten der Mischkörper aus isotropen Substanzen," Ann. Phys. **24**, 636–664 (1935).
47. M. Kahnert and A. Devasthale, "Black carbon fractal morphology and short-wave radiative impact: a modelling study," Atmos. Chem. Phys. **11**, 11745–11759 (2011).
48. M. Kocifaj, F. Kundracík, and G. Videen, "Optical properties of single mixed-phase aerosol particles," J. Quant. Spectrosc. Radiat. Transfer **109**, 2108–2123 (2008).
49. M. Schnaiter, C. Linke, O. Moehler, K.-H. Naumann, H. Saathoff, R. Wagner, U. Schurath, and B. Wehner, "Absorption amplification of black carbon internally mixed with secondary organic aerosol," J. Geophys. Res. **110**, D19204 (2005).
50. M. Kahnert, "Irreducible representations of finite groups in the T matrix formulation of the electromagnetic scattering problem," J. Opt. Soc. Am. A **22**, 1187–1199 (2005).

1. Introduction

Light absorbing carbon (LAC) aerosols, originating from burning of fossil fuel, biofuel, and biomass, are among the major anthropogenic radiative forcing agents in the atmosphere [1–3]. The radiative climate forcing impact of LAC is still poorly constrained, partly because of the high sensitivity of the aerosol optical properties (AOP) on the complex morphological properties of this class of aerosols.

In the following discussion, we refer to a mixture of aerosols, in which different chemical components are contained in physically separated particles, as an external mixture. Mixtures in which different chemical compounds are contained in the same particles are known as internal mixtures. The latter can be subdivided into materials in which the constituents are homogeneously mixed on the molecular level, and encapsulated geometries, in which non-soluble constituents, such as LAC, remain solid and are covered with other material.

Pure LAC aerosols are composed of an agglomeration of spherules, where the spherules are composed of incompletely graphitized para-crystalline carbon that can be partially oxidized. Both the composition and the morphology of LAC depend on types of fossil fuel or biomass source, the burning process, and the aging processes in the atmosphere [4]. The morphology of a fractal-like aggregates consisting of N_s monomers of radius a can be described by the scaling relation [5]

$$N_\mathrm{s} = k_0 \left(\frac{R_\mathrm{g}}{a} \right)^{D_\mathrm{f}}, \tag{1}$$

where D_f and k_0 are the fractal dimension and structural prefactor. The radius of gyration R_g of

#163542 - $15.00 USD Received 22 Feb 2012; revised 12 Apr 2012; accepted 12 Apr 2012; published 18 Apr 2012

the aggregate is defined as

$$R_{\mathrm{g}} = \sqrt{\frac{1}{N_{\mathrm{s}}} \sum_{i=1}^{N_{\mathrm{s}}} r_i^2}\,, \tag{2}$$

where r_i denotes the distance of the ith monomer from the aggregate's center of mass.

Simplified model particles, such as spheres or hollow spherical shells, do not correctly reproduce the optical properties of such complex fractal aggregates (e.g. [6]). Also, ad hoc approximations to Maxwell's equations, in which the electromagnetic scattering problem is solved by partially or completely neglecting electromagnetic interactions among the spherules, can introduce large errors in AOP computations (e.g. [7, 8]). Accurate results of both scattering and absorption properties of LAC aggregates can be obtained by use of numerically exact solution methods to Maxwell's equations, such as the superposition T-matrix method [9]. Recently, this method has been employed to compute AOP of LAC aggregates [10]. These computations covered the range of relevant aggregate sizes as well as wavelengths from the UV-C to the mid-IR. However, they were limited to externally mixed LAC.

As aerosols age in the atmosphere, LAC can become partially oxidized, and it can mix with other aerosol components by condensation. In the course of this aging process LAC becomes more hydrophilic. This typically happens on the time scale of a few hours [11, 12] up to a few days [1, 13, 14]. The aging process may also depend on the concentration of sulfuric acid [15]. Analysis of field measurements indicates that particles composed of internal mixtures of LAC, organic matter, and sulfate are frequently encountered in continental aerosols [16]. Coagulation can, in principle, also contribute to mixing of LAC with soluble compounds. In practice, however, condensation is, by far, the dominant mixing process.

Both aging [17] and wetting [18–21] of LAC often involves a collapse of the initially more fluffy aggregate structure to a more compact packing of the spherules. This morphological change can be described by an increase in the fractal dimension D_{f}. Both measurements and diffusion-limited cluster aggregation models suggest that freshly emitted LAC has a fractal dimension around D_{f}=1.82 and a structural prefactor of k_0=1.27 (e.g. [19, 22]). Studies with more advanced 3D measurement techniques based on electron tomography have been reported recently [23]. Such electron tomography measurements suggest somewhat higher values of the fractal dimension and lower values of the structural prefactor [4]. Thus measurements of fresh LAC near traffic sources yield fractal dimensions in the range D_{f}=2.1–2.3 with a median value D_{f}=2.2, and a structural prefactor in the range k_0=0.34–1.2 with a median k_0=0.71. Corresponding measurements of long-range transported, externally mixed LAC aerosols originating from different sources yield, on average, higher values of a fractal dimension in the range D_{f}=1.9–2.6 with a median D_{f}=2.4, and k_0=0.25–1.6 with a median k_0=0.67. The long-range transported aerosols were somewhat older than those observed near traffic sources. But they were still relatively fresh, since they had not yet mixed internally with sulfate or organic matter. However, their observed fractal dimensions agree with other studies of aged LAC aerosols, which report values of D_{f} in the range of 2.0–2.5 [19, 21].

The radius a of the carbonaceous monomers in the aggregates varies over a range of about 10–25 nm [7]. A value of a=25 nm has been reported to give good agreement of modelled single-scattering albedos with measurements [8]. This is consistent with field observations, which found a median value of about a=22 nm [16]. In the same field observations the number of monomers N_{s} has been observed to vary up to about N_{s}=800 [16]. The majority of LAC aggregates encapsulated by soluble compounds are found in the accumulation mode, i.e. the volume-equivalent radius R of these internally mixed aerosols lies typically in the range between 50–500 nm.

To compute the optical properties of chemically heterogeneous aerosols, such as mixtures of

#163542 - $15.00 USD Received 22 Feb 2012; revised 12 Apr 2012; accepted 12 Apr 2012; published 18 Apr 2012

LAC with weakly absorbing compounds, different simplifying assumptions about the aerosols' morphological properties have been tested. By far the crudest approximation is to ignore internal mixing, and to simply treat different chemical components as externally mixed aerosols. A slightly better, but still fairly simple treatment is the use of effective medium theory (EMT) [24, 25], which is based on describing the material as a homogeneous internal mixture of different chemical components. The main idea is to determine an effective refractive index for the internally mixed material. More realistic models account for the encapsulated geometries of aerosols containing both LAC and weakly absorbing compounds. The simplest encapsulated particle model is the concentric spherical core-shell model, consisting of a spherical LAC core and a concentric spherical coating of weakly absorbing material. The external mixture, homogeneous internal mixture, and encapsulated core-shell models predict distinctly different radiative forcing rates for LAC in global climate models [1]. It has been found that a carbon core encapsulated in a concentric soluble shell yields radiative forcing estimates that are 50% higher than those obtained with an external mixture model, and 40% lower than with a homogeneous internal mixture model [26]. This is consistent with results reported in [27, 28]. Coating of LAC with soluble material enhances absorption by a factor of about 1.5 as compared to freshly emitted, externally mixed LAC [27]. The amplification of absorption is, in general, dependent on the relative size of the LAC core and the weakly absorbing shell [27]. Note, however, that coating of LAC also increases the effectiveness of wet deposition, thus reducing the atmospheric lifetime of LAC, which, in turn, reduces the time-integrated radiative impact of LAC.

Field observations reveal that most encapsulated soot aggregates are located near the surface rather than at the center of the soluble coating. Numerical experiments have been performed to study the optical properties of spherical cores placed at arbitrary locations within a spherical shell of weakly absorbing material [29, 30]. For carbon cores with sulfate coatings, it was found that the absorption is more sensitive to the relative size of the core and the shell than to the position of the core within the shell. On the other hand, for very small carbon inclusions in large water droplets, absorption is significantly higher for centered than for off-center carbon inclusions. However, as remarked by Bond et al. [27], very small carbon cores are extremely rare under atmospheric conditions. These findings suggest that the position of the LAC core is of minor importance for modelling the optical and radiative properties of internally mixed LAC. On the other hand, a recent study based on a more realistic aggregate model with a soluble coating showed that off-center encapsulated soot aggregates can yield radiative forcing predictions that are as much as 20% less than those obtained with simple concentric core-shell models [31].

A recent investigation studied complex geometries of multiple soot particles encapsulated into a spherical host particle of weakly absorbing material [32]. The model geometries were based on field observations. Computations were performed with the discrete dipole approximation (DDA) [33]. Comparison of computed optical properties of the reference geometries to optical properties obtained with simpler model particles suggested that models based on, e.g., a simple core-shell geometry may give sufficiently accurate results. Although this study was limited to two encapsulated reference geometries, the results provide a promising basis for further investigations. Another recent study considered the optical properties of LAC aggregates attached to spherical soluble aerosol particles [34]. Such geometries, in which the LAC aggregate is touching the soluble particle, rather than being encapsulated by it, can result from coagulation. However, coagulation is mainly effective for scavenging of nucleation-mode particles by accumulation-mode aerosols. For mixing LAC aggregates with soluble compounds coagulation processes play a minor role in comparison to condensation processes. Thus, coagulated geometries are far less common than encapsulated geometries. We will therefore not consider such geometries in the present study.

#163542 - $15.00 USD Received 22 Feb 2012; revised 12 Apr 2012; accepted 12 Apr 2012; published 18 Apr 2012

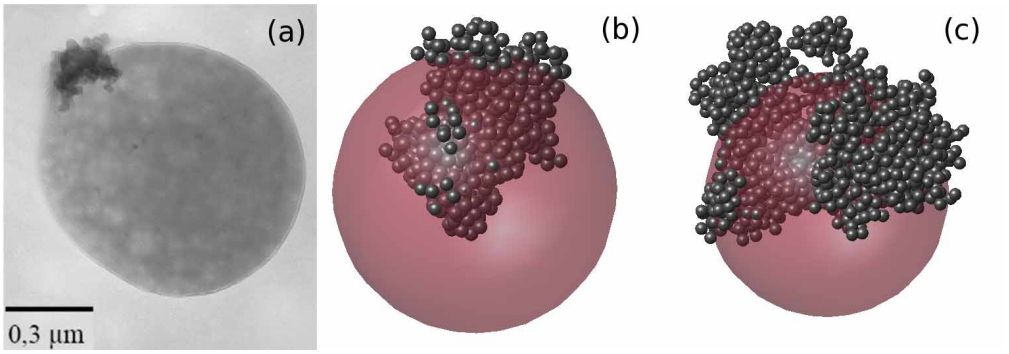

Fig. 1. (a) Electron micrograph of LAC aggregate encapsulated in sulfate shell. (Note that most of the aggregate is inside the sulfate shell, while only a small part is sticking out.) Examples of encapsulated aggregate models considered in this study with the following parameters: (b) $f = 0.07$, $R = 500$ nm, N_s=560, and (c) $f = 0.20$, $R = 500$ nm, N_s=1600.

For broadband AOP computations applicable to climate modelling, it is unavoidable to introduce simplifying assumptions about the morphology of LAC aerosols mixed with weakly absorbing aerosol compounds. Solving the light scattering problem for complex geometries requires the use of computationally demanding numerical methods, such as the DDA. Realistic encapsulated particles are characterized by LAC aggregates of varying size and geometry, as well as weakly absorbing material of varying size and chemical composition (thus varying effective refractive index). So the parameter space that needs to be considered is fairly large. It is therefore not possible to perform detailed DDA computations that cover the whole range of relevant sizes, wavelengths, LAC volume fractions, and chemical compositions of the weakly absorbing material. Rather, DDA computations have to be limited to considering a few representative cases, which can be used as benchmarks for testing simpler model particles. One often tries to employ isotropic model geometries, since light scattering computations are particularly fast for spherically symmetric particles. One goal of our investigation is to test the validity of such models for a sufficiently broad range of the relevant parameter space. As reference geometries we consider LAC aggregates encapsulated in a weakly absorbing shell. AOP computations for these complex reference geometries are performed by use of the DDA [9]. The main parameters we vary in this study are the sizes of the aerosol particles and the volume fraction of LAC. The reference computations will be compared to corresponding results obtained with simpler model geometries. The calculations are performed for one UV, one visible, and one IR wavelength. In the following section, the model geometries are introduced. Computational methods are presented and tested in Sect. 3. Results are presented and discussed in Sects. 4 and 5, respectively.

2. Model geometries

2.1. Reference geometries

We consider internally mixed, aged LAC aggregates with a more compact fractal structure. Figure 1 shows a micrograph of an LAC aggregate encapsulated in a sulfate shell, and two of the model geometries employed in this study. The choice of our model particles is mainly based on most recent results reported in Refs. [16, 31]. We compute the optical properties of LAC aggregates internally mixed with soluble material for the following choices of parameters.

- Two different LAC volume fractions of f=7% and 20%;

#163542 - $15.00 USD Received 22 Feb 2012; revised 12 Apr 2012; accepted 12 Apr 2012; published 18 Apr 2012

- A constant monomer radius of 25 nm [8, 16];
- A fixed fractal dimension and structural prefactor of D_f=2.6 and k_a=1.2 [16];
- Encapsulated geometries, in which the distance D_i between the centers of mass of the LAC aggregate and the soluble shell is given by D_i/R_{shell}=0.5 [31], where R_{shell} is the radius of the soluble shell;
- The particle sizes considered for the two different volume fractions are given in Table 1;
- Three different wavelengths, 304.0 nm, 533.2 nm, and 1010.1 nm. These wavelengths are the mid-points of the second, fourth, and sixth band of the radiation model in the latest versions of the Integrated Forecasting System (IFS), which is the atmospheric circulation module in the Earth-system climate model EC-EARTH (http://ecearth.knmi.nl).

The soluble material is assumed to be sulfate. The particle sizes we consider covers the typical range of internally mixed LAC-soluble aerosols. The refractive indices we assumed in our computations are listed in Table 2. The values for LAC are based on measurements in [35]. Those for SO_4 are based on the OPAC database [36].

Table 1. Number of monomers N_s in the LAC aggregates and corresponding volume-equivalent radii R of the internally mixed aerosols (where the volume of both the LAC and the soluble material has been accounted for).

f=7%		f=20%	
N_s	R [nm]	N_s	R [nm]
4	96	13	101
36	200	102	200
121	300	346	300
287	400	819	400
560	500	1600	500

Table 2. Refractive indices m of LAC and sulfate at three wavelengths λ.

λ [nm]	m (LAC)	m (SO_4)
304.0	1.33+0.75i	$1.47+10^{-8}$i
533.2	1.76+0.63i	$1.43+10^{-8}$i
1010.1	1.92+0.56i	$1.42+1.75\cdot10^{-4}$i

2.2. Simplified model geometries

In addition to the realistic model particle morphologies, we consider four classes of simplified model geometries, which are illustrated in Fig. 2.

(a) Externally mixed LAC and soluble particles, each assumed to be homogeneous, volume-equivalent spheres. The radii R_{LAC} and R_{SO_4} can be obtained from the total radius R and the LAC volume fraction f, i.e.

$$R_{LAC} = f^{1/3}R \quad (3)$$

$$R_{SO_4} = (1-f)^{1/3}R \quad (4)$$

#163542 - $15.00 USD Received 22 Feb 2012; revised 12 Apr 2012; accepted 12 Apr 2012; published 18 Apr 2012

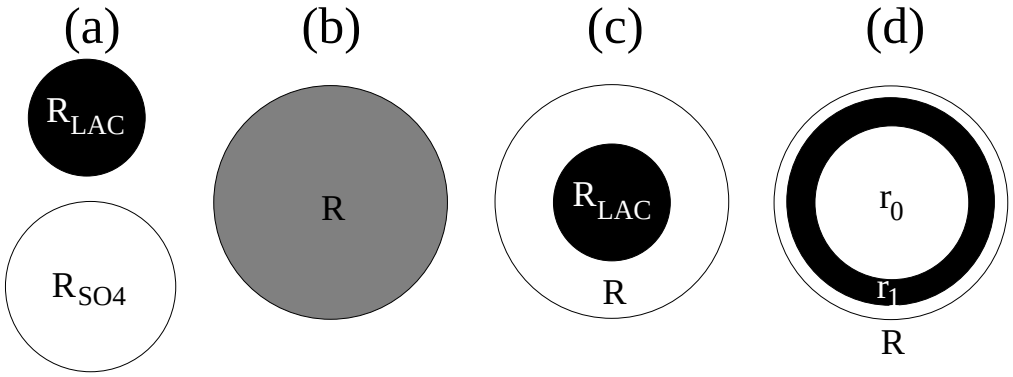

Fig. 2. (a) External mixture, (b) homogeneous internal mixture, (c) core-shell, and (d) core-shell-shell model.

(b) Homogeneous internal mixtures of LAC and soluble compounds. The effective refractive index is computed by effective medium theory [24].

(c) Inhomogeneous internal mixture, described by a concentric spherical core - shell model. The LAC core has radius R_{LAC}, and the total size of the particle is R.

(d) Concentric spherical core-shell-shell model. The inner core of soluble material has radius r_0, the LAC shell extends from r_0 to r_1, and the outer soluble shell from r_1 to the outer radius R. The core radius r_0 is a free parameter, and the radius r_1 is determined by the volume fraction and the total size of the particle (as discussed in Sect. 4).

3. Methods and preliminary tests

The electromagnetic scattering computations for the complex coated aggregate particles are performed by using the discrete dipole approximation (DDA) [33]. We use the DDSCAT implementation by Draine and Flatau [37]. The DDA is a volume-integral equation method, which is based on discretizing the volume of the scatterer, and assuming that the electromagnetic field is constant within each volume cell. In that case each volume cell scatters just like a dipole. This assumption is valid if each volume cell is small compared with the wavelength of light. In practice, this implies that $|m|kd$ should be sufficiently small, where m is the refractive index of the material, $k = 2\pi/\lambda$ is the wavenumber, and d denotes the dipole spacing. The smaller d, the larger the total number of dipoles employed for representing the target. The computation time in the DDA increases rapidly with increasing number of dipoles.

Representing the target by a cubic grid of volume elements, each scattering like a dipole, can introduce two different sorts of errors. First, if the size of the volume cells, i.e. the dipole spacing, is not chosen sufficiently small, then the dipole-approximation may not be valid, and the DDA will give non-physical results. Second, the discretization may be too coarse to accurately approximate the actual geometry of the scatterer. This is especially a concern for complex geometries, such as LAC aggregates composed of small spherules, in which each spherule needs to be represented by a sufficiently large number of dipoles.

Although there do exists some general guidelines for choosing the dipole spacing in the DDA, application of this method to morphologically complex particles should be preceded by some tests of the validity of the method. First, we compared computations for pure aggregates to numerically exact computations with the superposition T-matrix method (STM) [9]. To this end, we amended the STM code by Mackowski and Mishchenko [9] to compute the polarized

#163542 - $15.00 USD Received 22 Feb 2012; revised 12 Apr 2012; accepted 12 Apr 2012; published 18 Apr 2012

differential scattering cross section of aggregates in a fixed orientation, since this quantity is highly sensitive to numerical inaccuracies. In parallel, we tested the accuracy of the DDA results with the reciprocity condition (e.g. [38, 39]). We required that this condition be fulfilled with an error less than 3%. Note that this is a very sensitive indicator of the accuracy of T-matrix calculations, but it is still not clear to what extent the reciprocity test can be used to check the accuracy of DDA results. In conjunction with certain polarizability models the DDA automatically fulfills the reciprocity condition. In such cases, this approach cannot be used as an accuracy test. We performed reciprocity tests in conjunction with the polarizability model described in [40], which does not automatically satisfy the reciprocity condition. By decreasing the dipole spacing, one obtains an increasingly better agreement with the numerically exact T-matrix results, and, well correlated to that, an increasingly better fulfillment of the reciprocity condition. This seems to indicate that the reciprocity test can, indeed, serve as a useful supplementary test in this case. We therefore repeated the reciprocity tests for the encapsulated aggregate models, for which we do not have numerically exact T-matrix results as a benchmark. A different accuracy test for irregular targets in DDA computations, which is based on two different ways of computing the scattering cross section, has been proposed in [41].

As a result of these tests we found that the dipole spacing d should be chosen such that $|m|kd \lesssim 0.32$, where m is the complex refractive index, and $k = 2\pi/\lambda$ denotes the wavenumber. In the calculations, we used one dipole spacing d_1 that satisfies this condition for a wavelength of $\lambda = 231.6$ nm, and another dipole spacing d_2 that satisfies the condition for $\lambda = 533.2$ nm. The former wavelength is the mid-point of the lowest band in the IFS radiation scheme. d_1 has been used for the computations at $\lambda = 304.0$ nm, d_2 has been used at $\lambda = 533.2$ and 1010.1 nm. So the condition $|m|kd \lesssim 0.32$ is fulfilled for all three wavelengths. The number of dipoles per monomer is $N_d/N_s = 51$ for d_1 and $N_d/N_s = 22$ for d_2 (where N_d is the number of dipoles, and N_s is the number of monomers in the aggregate).

In the DDA, averaging the optical properties over orientational angles has to be performed numerically. It is important to test that the ensemble-averaged results have converged with respect to the number of discrete angles N_o. We varied N_o up to more than 23000 and analyzed the orientation-averaged phase function and degree of linear polarization. For pure aggregates we performed both relative comparisons of DDA results for different N_o, as well as comparisons against T-matrix results. Orientation-averaging is done analytically in T-matrix methods, so these results are numerically exact benchmarks. For encapsulated aggregates, the STM code cannot be applied, so we only performed relative comparisons of DDA results for different N_o. Choosing $N_o = 864$ was sufficient for obtaining accurate orientation-averaged results at all wavelengths, for all particle sizes, and for both pure and encapsulated aggregates.

Mie calculations for homogeneous spheres were performed with a program by Mishchenko [42]. For computing light scattering by core-shell particles we used a code by Wiscombe based on [43]. Optical properties of core-shell-shell particles were computed with a program for multi-layer spheres described in [44].

For internal mixtures of LAC and sulfate modelled by homogeneous spheres, we considered different approaches for computing the effective refractive index $m_{\text{eff}} = \sqrt{\varepsilon_{\text{eff}}}$ of the internally mixed particle, where ε_{eff} denotes the effective electric permittivity. In the Maxwell-Garnett mixing rule [45], it is assumed that inclusions with a permittivity ε_1 and volume fraction f_1 are embedded in a host matrix with permittivity ε_2. The effective permittivity is obtained from

$$f_1 \frac{\varepsilon_1 - \varepsilon_2}{\varepsilon_1 + 2\varepsilon_2} = \frac{\varepsilon_{\text{eff}} - \varepsilon_2}{\varepsilon_{\text{eff}} + 2\varepsilon_2}. \tag{5}$$

In the Bruggemann mixing rule [46], the two materials are assumed to be embedded in a host

#163542 - $15.00 USD Received 22 Feb 2012; revised 12 Apr 2012; accepted 12 Apr 2012; published 18 Apr 2012

medium with an effective permittivity $\varepsilon_{\rm eff}$ given by

$$f_1 \frac{\varepsilon_1 - \varepsilon_{\rm eff}}{\varepsilon_1 + 2\varepsilon_{\rm eff}} + f_2 \frac{\varepsilon_2 - \varepsilon_{\rm eff}}{\varepsilon_2 + 2\varepsilon_{\rm eff}} = 0, \tag{6}$$

where $f_2 = 1 - f_1$ is the volume fraction of the second material. Thus the Bruggemann rule treats the two material more symmetrically. It seems most natural to use the Maxwell-Garnett rule for a mixture of LAC with sulfate, and to treat LAC as inclusions. However, we also experimented with the Bruggemann rule, and with the inverse Maxwell-Garnett rule (treating sulfate as inclusions in an LAC matrix). Among climate modelers and atmospheric chemists it is quite popular to compute the effective refractive index of homogeneous internal mixtures with simple volume-mixing rules. Such mixing rules are purely empirical without any underlying physical assumptions about the form of mixture. More physical approaches, such as the Maxwell-Garnett or Bruggemann mixing rules, seem to be largely unknown in these communities. Note that there are different forms of volume-mixing rules for computing $\varepsilon_{\rm eff}$ (e.g. [24]), such as

$$\varepsilon_{\rm eff} = f_1\varepsilon_1 + f_2\varepsilon_2, \tag{7}$$

$$\sqrt{\varepsilon_{\rm eff}} = f_1\sqrt{\varepsilon_1} + f_2\sqrt{\varepsilon_2}. \tag{8}$$

We also tested both of these volume-mixing rules and gauged their performance by comparing the results to the reference computations for encapsulated LAC aggregates.

4. Results

Figures 3–8 show optical properties as a function of particle size computed for the three different wavelengths λ and two LAC volume fractions f. For each particle size, we performed DDA computations for five stochastic realizations of the aggregates with prescribed fractal parameters . The results are indicated in the figures by symbols. By inspecting Figs. 3–8, we find, as a general trend, that (a) the extinction cross section $C_{\rm ext}$, (b) the total scattering cross section $C_{\rm sca}$, (c) the absorption cross section $C_{\rm abs} = C_{\rm ext} - C_{\rm sca}$, (d) the single-scattering albedo $\omega = C_{\rm sca}/C_{\rm ext}$, (e) the asymmetry parameter g, and to some extend also (f) the backscattering cross section $C_{\rm bak}$ do not vary much among the five stochastically generated geometries. This verifies that these optical properties are reasonably well constrained by defining classes of geometries with prescribed $D_{\rm f}$, k_0, a, N_s, R, and $D_{\rm i}/R_{\rm shell}$.

In the last row we show (g) the backscattering linear depolarization ratio δ_L, and (h) the backscattering circular polarization ratio δ_C. The main reason why we included these quantities in the plots was to illustrate that δ_L and δ_C can vary considerably among different stochastic realizations of the encapsulated aggregate geometries, especially for a volume fractions of f =20%. Clearly, none of the model particles considered in this study is suitable for mimicking the backscattering depolarization ratios, since particles with spherical symmetry that are composed of material with isotropic dielectric and magnetic properties never depolarize light.

Results for $\lambda = 304.2$ nm and $f = 7\%$ are presented in Fig. 3. External mixtures of LAC and sulfate spheres perform poorest, as they strongly underestimate both absorption and scattering. Coating an LAC core with a sulfate shell enhances absorption. This can be understood in terms of focusing of the internal field onto the LAC core, thus allowing more electromagnetic energy to interact with the absorbing core. However, the core-shell model still significantly underestimates $C_{\rm abs}$. The reason is that the electromagnetic field is unable to penetrate deeply into a massive, spherical LAC core. In the encapsulated aggregate model the LAC mass is distributed such that more absorbing material can interact with the electromagnetic field, thus increasing $C_{\rm abs}$. In the homogeneous internal mixture model with Maxwell-Garnett EMT, the LAC material is evenly distributed throughout the sulfate host particle. This model overestimates $C_{\rm abs}$,

#163542 - $15.00 USD Received 22 Feb 2012; revised 12 Apr 2012; accepted 12 Apr 2012; published 18 Apr 2012

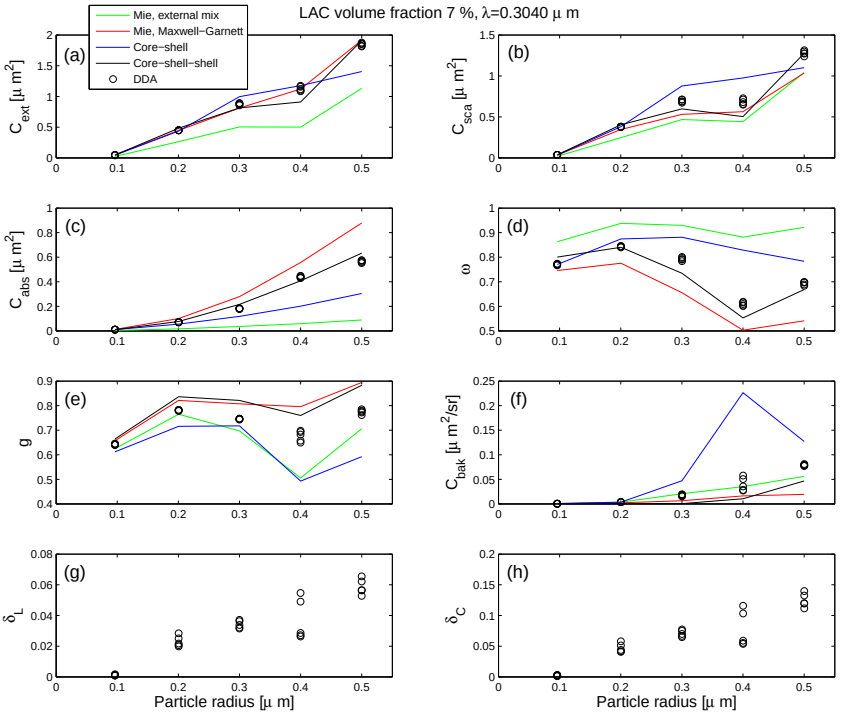

Fig. 3. Optical properties for $\lambda = 304.2$ nm and f =7%, computed for 5 stochastic realizations of encapsulated aggregates (symbols), externally mixed LAC and sulfate spheres (green line), homogeneous spheres with an effective refractive index based on Maxwell-Garnett EMT (red line), LAC cores with sulfate shell (blue line), and sulfate cores with LAC inner shell and sulfate outer shell (black line).

because it underestimates the screening (i.e. "shading") of part of the LAC mass from interacting with the electromagnetic field. However, it is interesting to note that the Maxwell-Garnett EMT model seems to give better results than the putatively more realistic core-shell model. Neither the external-mixture, nor the core-shell, nor the Maxwell-Garnett models give very good results for the asymmetry parameter g and the single-scattering albedo ω.

Inspection of C_{abs} in Figs. 3–8 shows that there are some minor variations of the situation we just discussed; but as a general trend we can state that the core-shell model mostly underestimates C_{abs}, while the Maxwell-Garnett EMT model mostly overestimates C_{abs}. Based on the physical explanation given above for these phenomena, we need to find a model particle that distributes the LAC mass less compactly than the core-shell model, but not as evenly as the homogeneous internal mixture model based on Maxwell-Garnett EMT. Thus we introduce the following idea. Consider a particle consisting of three concentric spherical layers, a sulfate core of radius r_0, an LAC shell extending from r_0 to r_1, and a sulfate shell from r_1 to the outer radius R. The radius r_0 is a free parameter, but the radius r_1 is constrained by the LAC volume fraction. Let R_{LAC} denote the volume-equivalent radius of the LAC material in the internally

#163542 - $15.00 USD Received 22 Feb 2012; revised 12 Apr 2012; accepted 12 Apr 2012; published 18 Apr 2012

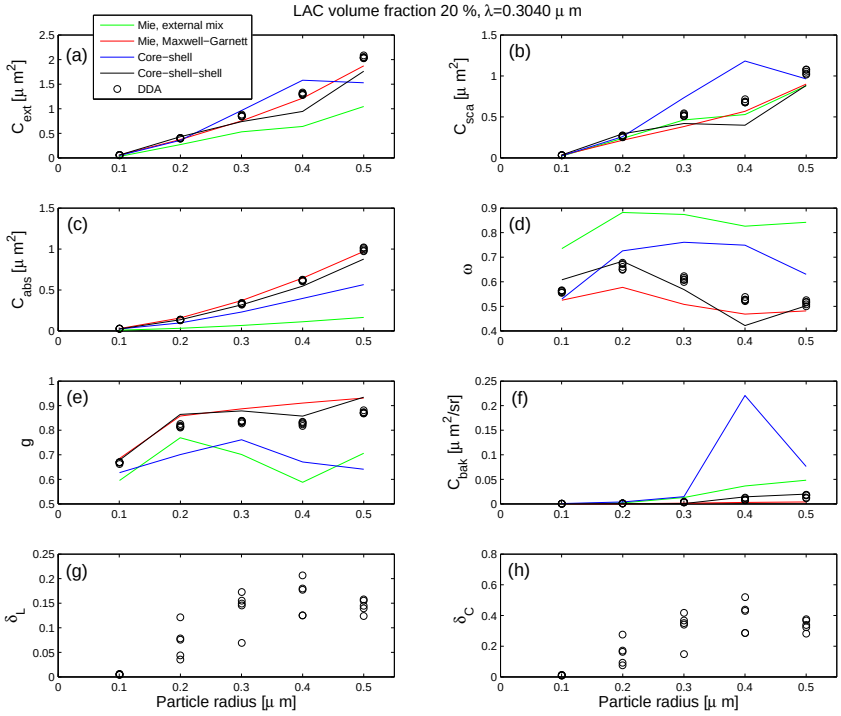

Fig. 4. As Fig. 3, but for $\lambda = 304.0$ nm and f =20%.

mixed particle. Then r_1 has to be such that $r_1^3 - r_0^3 = R_{\mathrm{LAC}}^3$. Using Eq. (3) we obtain

$$r_1 = \left(fR^3 + r_0^3\right)^{1/3}. \tag{9}$$

We investigated the agreement of the optical properties computed with this model for different choices of r_0. The motivation of investigating this model was to obtain better values of C_{abs}, which was poorly represented by the other model particles. However, we found that the core-shell-shell model generally tends to perform better than the other models for ω and g as well. Although the optimum choice of r_0 can slightly vary among different optical properties and different values of λ, f, and R, using $r_0 = 0.9R_{\mathrm{SO_4}}$ gives in most cases remarkably good agreement between the reference results for encapsulated aggregates and the core-shell-shell model, where $R_{\mathrm{SO_4}}$ has been defined in Eq. (4). The results for the core-shell-shell model with this choice of r_0 are represented by the black lines in the figures.

For f =7% and $\lambda = 304.2$ nm (Fig. 3), the Maxwell-Garnett EMT model reproduces C_{ext} very well. However, inspection of C_{sca} and C_{abs} shows that this is caused by a rather fortuitous error cancellation. C_{sca} is underestimated, and C_{abs} is overestimated. As a results this model predicts too low values of ω. The core-shell-shell model gives reasonable results for C_{sca} and very accurate results for C_{abs}, therefore a better estimate of ω. Both models give very similar results for g. For f =20% and $\lambda = 304.2$ nm (Fig. 4), the Maxwell-Garnett EMT model gives slightly more accurate results for C_{ext}, but, except for R =400 nm, less accurate results for ω than the core-shell-shell model. Again, the results for g are rather similar.

#163542 - $15.00 USD Received 22 Feb 2012; revised 12 Apr 2012; accepted 12 Apr 2012; published 18 Apr 2012

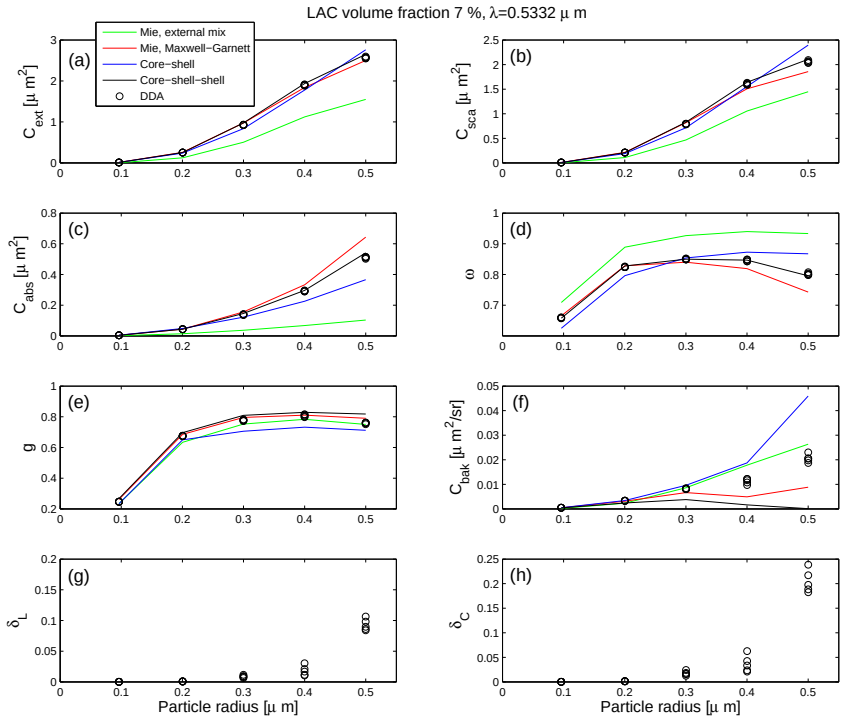

Fig. 5. As Fig. 3, but for $\lambda = 533.2$ nm and f =7%.

The most important cases are those with $\lambda = 533.2$ nm, as this wavelength lies close to the maximum of the solar spectrum. Thus these cases are most important for estimating the radiative forcing effect of LAC. For f =7% (Fig. 5) the core-shell-shell model gives nearly perfect estimates of $C_{\rm ext}$, $C_{\rm sca}$, $C_{\rm abs}$, and ω. The Maxwell-Garnett EMT model, again, underpredicts $C_{\rm sca}$ and overpredicts $C_{\rm abs}$, which results in too low values of ω. Both models give similar values of g that agree reasonably well with the reference calculations for the encapsulated aggregates. Very similar observations can be made for f =20% (Fig. 6).

For $\lambda = 1010.1$ nm and f =7% and 20% (Figs. 7 and 8), both the Maxwell-Garnett EMT and the core-shell-shell model give almost identical results that reproduce the reference computations very well.

We also tested the performance of different effective medium approaches (not shown in the figures). To this end, we performed Mie calculations with effective refractive indices computed with the Maxwell-Garnett rule, the Bruggemann rule, and the inverse Maxwell-Garnett rule. We also tested two volume-mixing rules given in Eqs. (7) and (8). In most cases, the Maxwell-Garnett approach gave the closest agreement with the reference computations. The Bruggemann mixing rule performed almost equally well, while the inverse Maxwell-Garnett rule worked slightly worse. The volume-mixing rules worked reasonably well at UV wavelengths, and at visible and IR wavelengths the volume-mixing rule given in Eq. (8) was only slightly worse than the Maxwell-Garnett rule. However, the volume-mixing rule given in Eq. (7) results in a strong underestimation of $C_{\rm sca}$, an overestimation of $C_{\rm abs}$, and, consequently, and underestimation of

#163542 - $15.00 USD Received 22 Feb 2012; revised 12 Apr 2012; accepted 12 Apr 2012; published 18 Apr 2012

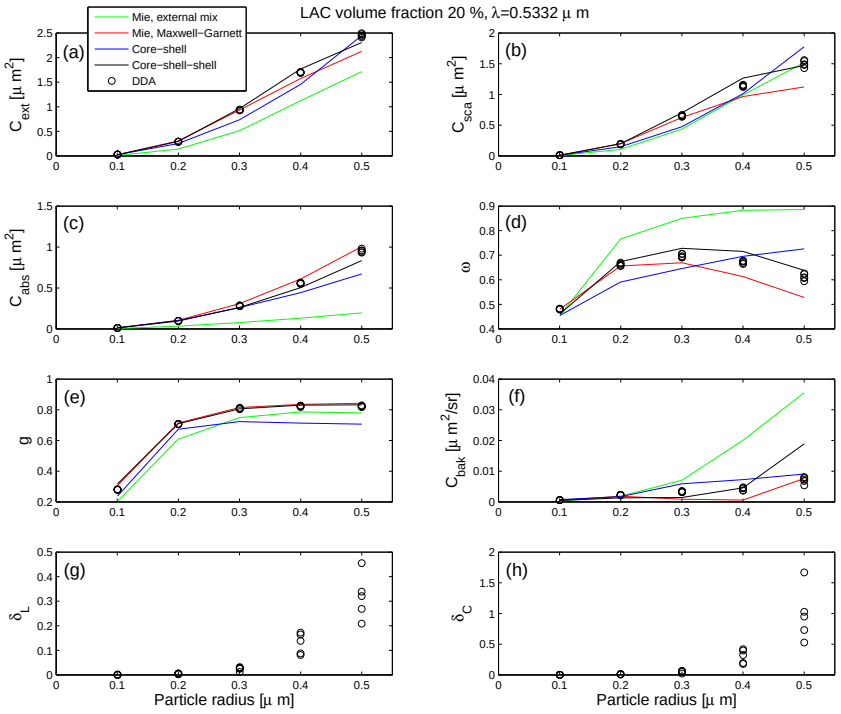

Fig. 6. As Fig. 3, but for $\lambda = 533.2$ nm and f =20%.

ω. This alerts us that simple, non-physical effective medium approximations can introduce large errors unless they are properly tested. It is usually safer to use more physical EMT approaches.

5. Discussion and conclusions

The mixing state of light absorbing carbon with other aerosol components profoundly impacts the radiative heating effect of LAC [1]. It has been hypothesized that a core-shell model based on an LAC core encapsulated with a soluble shell is more physical than models based on external mixtures or homogeneous internal mixtures of LAC with organic and secondary inorganic aerosol components [26]. It seems reasonable to assume that the physically more realistic core-shell model produces more accurate aerosol optical properties. However, the results of our study do not support this conjecture. We do find that the core-shell model clearly outperforms the external mixture model. But it does, in general, produce less accurate results than the homogeneous internal mixture model in conjunction with Maxwell-Garnett effective medium theory.

This is a striking and, at first sight, unexpected result. However, it can be understood in similar terms as the optical properties of pure LAC aggregates. It has been shown earlier that aggregates of small LAC spherules give significantly larger extinction and absorption cross sections than compact LAC spheres [10, 47]. As explained in the previous section, the electromagnetic field cannot penetrate deeply into a massive sphere of highly absorbing material. As a result, much of the mass inside an LAC sphere does not contribute to the absorption of elec-

#163542 - $15.00 USD Received 22 Feb 2012; revised 12 Apr 2012; accepted 12 Apr 2012; published 18 Apr 2012

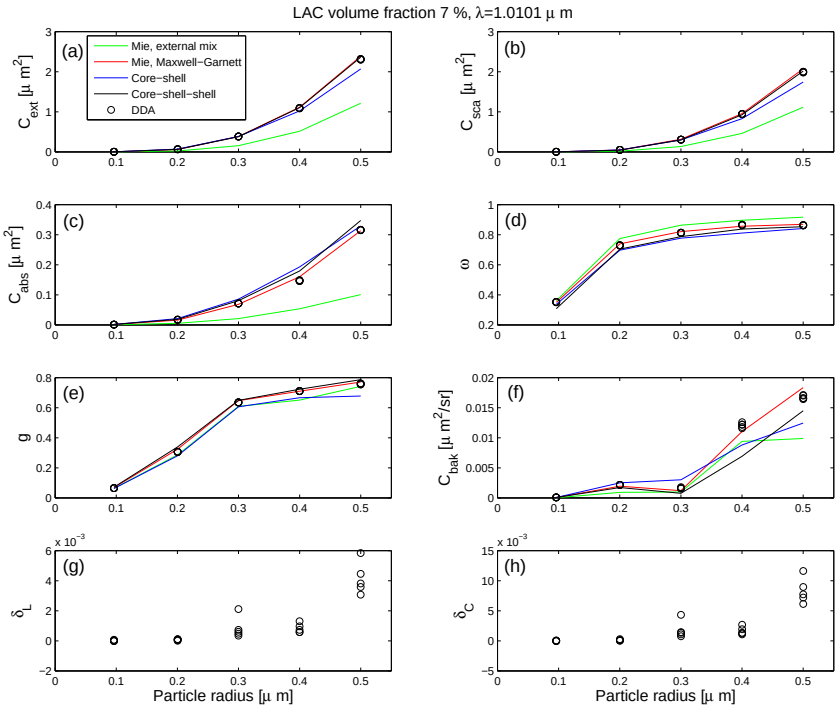

Fig. 7. As Fig. 3, but for $\lambda = 1010.1$ nm and f =7%.

tromagnetic energy. We encounter a similar problem in the core-shell model. The massive LAC core allows only a fraction of its mass to interact with the electromagnetic field. By contrast, the carbonaceous material in an encapsulated aggregate is distributed such that a much larger fraction of the mass can contribute to light absorption. Remarkably enough, this is even the case for aggregates with a fractal dimension as high as $D_{\rm f} = 2.6$. Note that this fractal dimension is at the upper end of the range that has been observed in field measurements of aged aerosols, in which the initially lacy fractal structure has significantly collapsed during the aging process of LAC in the atmosphere. Despite this high value of $D_{\rm f}$, a considerably higher fraction of the mass in the aggregate contributes to the mass absorption cross section than in a compact sphere. This is the physical reason why the core-shell model significantly underestimates $C_{\rm abs}$ of realistic encapsulated LAC aerosols. Thus this model is, to be sure, more physical from the point of view of aerosol chemistry and aerosol dynamics, but it is not realistic from the point of view of aerosol optics. The homogeneous internal mixture model, on the other hand, distributes the black carbon mass too evenly within the soluble host particle. It therefore overestimates $C_{\rm abs}$ in comparison to the morphologically realistic encapsulated aggregate model. This is particularly evident for visible wavelengths. However, the error introduced by the homogeneous internal mixture model in conjunction with Maxwell-Garnett EMT is significantly smaller than that caused by the core-shell model. Despite the reasonable performance of the Maxwell-Garnett approach in the case studies we considered, it is usually advised to use EMT-based approaches with caution. In general, the accuracy of effective medium approaches is difficult to predict,

#163542 - $15.00 USD Received 22 Feb 2012; revised 12 Apr 2012; accepted 12 Apr 2012; published 18 Apr 2012

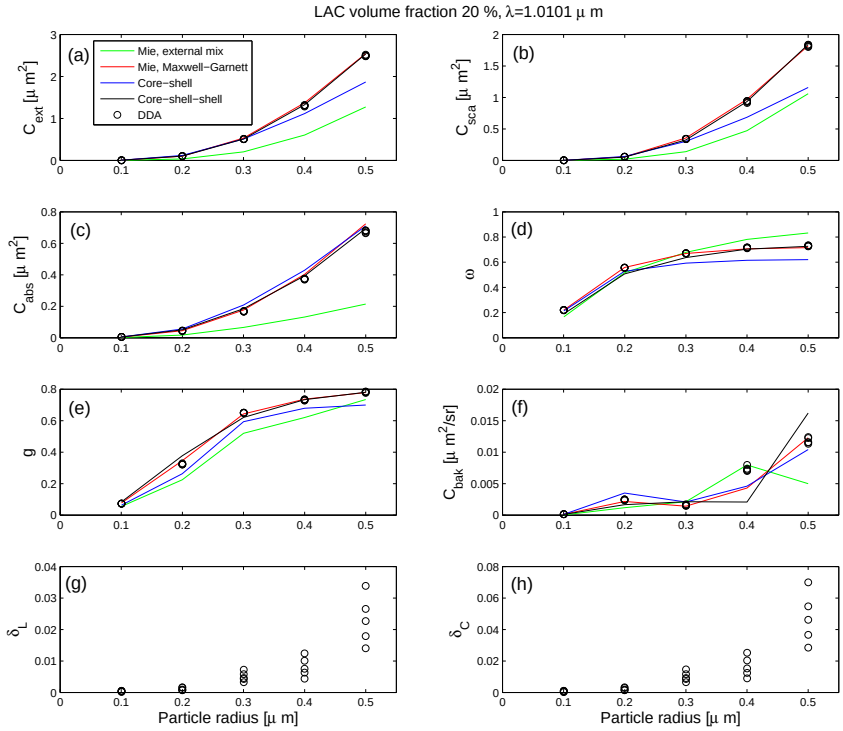

Fig. 8. As Fig. 3, but for $\lambda = 1010.1$ nm and f =20%.

and it depends on the morphology and relative size of the inclusion as well as on the single-scattering property of interest [28, 48].

It is interesting to note that a recent investigation of laboratory-generated LAC aggregates coated with secondary organic substances [49] found that a simple core-shell model does reproduce the absorption cross section of the reference particles reasonably well. A possible reason is that the fractal structure of the laboratory-generated LAC particles was even more strongly compacted than that of the particles we considered in our study. However, it has also been reported in the same paper [49] that the core-shell model does not accurately reproduce the single-scattering albedo, the Ångström exponent, and the hemispheric backscattering ratio of the coated LAC aggregates.

As expected, the external mixture model produces the least accurate results in our study. On the one hand, it suffers from the same problem as the core-shell model by underestimating the amount of LAC mass that interacts with the external electromagnetic field. On the other hand, the core-shell model does, at least, mimic the fact that a coating of soluble material increases the physical cross section of a particle and focuses some of the incident electromagnetic energy onto the LAC core, thus enhancing the absorption and scattering cross sections. The external mixture model neglects this effect.

We propose a compromise between the two extremes represented by the core-shell and the homogeneous internal mixture models. The idea is to retain the spherical symmetry, while distributing the LAC mass such that the amount of absorbing material that interacts with the

#163542 - $15.00 USD Received 22 Feb 2012; revised 12 Apr 2012; accepted 12 Apr 2012; published 18 Apr 2012

electromagnetic field is higher than in the core-shell model, and lower than in the homogeneous internal mixture model. This leads us to a core-shell-shell model, in which the core and the outer shell consist of soluble material, and the inner shell consists of LAC. The total carbon mass and the total mass of soluble material is fixed by the particle size and the volume fraction. The best overall agreement between the core-shell-shell model and the encapsulated aggregate reference results is obtained for a core radius r_0 given by $r_0 = 0.9R_{SO_4}$, where R_{SO_4} is the volume-equivalent radius of the total soluble material in the particle. It would, in principle, be possible to achieve further improvements by fine-tuning the choice of r_0 for each wavelength and volume fraction. However, the choice proposed here provides a simple and robust model that, on average, provides more accurate estimates of C_{ext}, C_{abs}, ω, and g than the homogeneous internal mixture and the core-shell models. The good performance of the core-shell-shell model is most pronounced at visible wavelengths, which are most important for obtaining accurate estimates of the short-wave radiative forcing effect of LAC. Also, by contrast to EMT-based models, the core-shell-shell model shares with the core-shell model the advantage of representing the particle by an encapsulated geometry that bears at least some resemblance to a realistic internal mixture of LAC with sulfate.

All of the simplified model particles considered here are spherically symmetric. Exploiting particle symmetries in solving the electromagnetic scattering problem can save several orders of magnitude in computation time [50]. However, symmetry assumptions constitute a drastic simplification. Our results confirm that such simplifications are justifiable only if we want to compute those optical properties that are relevant for climate forcing computations, such as C_{ext}, ω, and g. In remote sensing applications we are often interested in differential scattering properties, i.e. in the angular distribution of the scattered intensity and polarization. Our results indicate that it is considerably more challenging to reproduce the magnitude and size-dependence of the backscattering cross section C_{bak}. Also spherically symmetric particles invariably predict zero linear and circular backscattering depolarization, while encapsulated aggregates, can give quite high values of δ_L and δ_C. The model particles discussed here are therefore limited to climate applications and should not, without extensive additional tests, be applied in remote sensing studies.

Acknowledgments

B. Draine, D. Mackowski, M. Mishchenko, W. Wiscombe, and Z. Wu are acknowledged for making their respective light scattering programs publicly available. M. Kahnert acknowledges funding from the Swedish Research Council (projects 621-2008-4387 and 621-2011-3346). T. Nousiainen and H. Lindqvist acknowledge funding by the Academy of Finland (contract 125180). Two anonymous reviewers are acknowledged for helpful suggestions.

#163542 - $15.00 USD Received 22 Feb 2012; revised 12 Apr 2012; accepted 12 Apr 2012; published 18 Apr 2012